Asymmetrical Planetary Nebulae II: From Origins to Microstructures
ASP Conference Series, Vol. 199, 2000
J.H. Kastner, N. Soker, & S. Rappaport, eds.

Properties of Proto–Planetary Nebulae

Margaret Meixner

University of Illinois, Dept. of Astronomy, MC-221, 1002 W. Green St., Urbana, IL 61801

Abstract. This review describes some general properites of proto-planetary nebulae with particular emphasis on the recent work of morpholgical studies. The weight of observational evidence shows that proto-planetary nebulae (PPNe) are most certainly axisymmetric like planetary nebulae. Recent work suggests two subclasses of PPNe optical morphology, DUst-Prominent Longitudinally-EXtended (DUPLEX) and Star-Obvious Low-level Elongated (SOLE). Radiative transfer models of an example DUPLEX PPN and SOLE PPN, presented here, support the interpretation that DUPLEX and SOLE are two physically distinct types of PPNe. The DUPLEX PPNe and SOLE PPNe may well be the precursors to bipolar and elliptical PNe, respectively.

1. What is a Proto-Planetary Nebula?

The proto-planetary nebula (PPN;a.k.a. post-AGB or pre-PN) stage of evolution immediately precedes the planetary nebula (PN) stage. The lifetime for this phase is $\stackrel{<}{\sim}$ 1000 years and marks the time from when the star was forced off the asymptotic giant branch (AGB) by intensive mass loss to when the central star becomes hot enough ($T_{eff} \sim 3 \times 10^4$ K) to photoionize the neutral circumstellar shell (Kwok 1993). We refer the reader to Kwok (1993) for a comprehensive review of PPN. For short recent reviews, see Hrivnak (1997) and van Winckel (1999). In this short review, I summarize the basic properties of PPN but focus primarily on the morphological studies because there have been numerous morphological studies in the past few years and because this particular conference is focused on morphology.

2. General Characteristics of PPN

PPN are like PN in that the central star illuminates a detached circumstellar shell, however, we observe PPN using quite different techniques. Because PPN do not have ionized gas, we can not use the optically bright emission lines or radio free-free continuum commonly used for studies of PN. Instead tracers of dust and neutral gas are employed. In fact, PPN are identified as stars of spectral type B-K, luminosity class I with infrared excesses. These infrared excesses arise from the circumstellar dust which was originally created in the AGB wind. They emit broad ($\sim$20 km s^{-1}), parabolic or double–horned lines of CO rotational lines and

OH maser lines indicative of a remnant AGB circumstellar shell. These broad lines distinguish these PPN from pre-main sequence and Vega-excess stars which also have infrared excesses but typically narrower or non-existent molecular lines.

Candidates for PPN are discovered using infrared sky surveys. One of the most famous PPN, AFGL 2688 (a.k.a the Egg Nebula), was discovered by Ney et al. (1975) in an infrared sky survey done by the airforce. Studies using the IRAS all sky survey have used two approaches to identify candidates. One way is to use IRAS colors ([25]-[60] vs. [12]-[25]), mark the locations of known AGB stars and PN and choose PPN candidates from the regions in between (van der Veen, Habing & Geballe 1989; Hrivnak, Kwok & Volk 1989; Hu et al. 1993). The second way is to cross correlate the IRAS catalog with optical star catalogs and choose objects in common (Oudmaijer et al. 1992).

Several initial followup studies focused on ground based photometry observations and models of the spectral energy distributions (SEDs) of these PPN candidates. Van der Veen et al. (1989) identified four types of SEDs which they attributed to optical depth differences in the dust shells. Type I has a flat spectrum from 4 to 25 μm with a steep fall off at short wavelengths. Type II have a maximum near 25 μm and a gradual fall-off to shorter wavelengths. Type III have a maximum near 25 μm, a steep fall off at shorter wavelengths to a plateau between 1 and 4 μm. Type IV have two distinct maxima, one near 25 μm and the second at $\lambda < 2$ μm. Hrivnak & Kwok (1991) suggested that the 21μm PPN were quite similar to objects like AFGL 2688 except for viewing angle based on the differences in their SEDs. The 21μm PPN have a Type IV SED while AFGL 2688 has a Type III SED and we could be viewing the 21μm PPN down the poles while we view AFGL 2688 edge-on.

3. Morphologies

The study of PPN morphologies offers us insight on the axisymmetric PN issue because they are the missing link between two well studied groups: PN and AGB stars. Moreover, their morphologies are relatively pristine fossil records of the AGB mass loss process because shaping by the hot, fast stellar wind of a PN nucleus has probably not occured (see Schonberner in this volume). Hence we can determine "initial conditions" for the interacting winds models. Figure 1 shows our working model for a PPN circumtellar shell based on the observed evidence that most PN are axially symmetric (e.g. Balick 1987) while the outer shells of AGB circumstellar shells are spherically symmetric (e.g. Neri et al. 1998). In the PPN fossil record, radial distance directly corresponds to time. The maximum radius, R_{max} marks when the mass loss began. As we move inwards, we see the spherically symmetric shell created by the AGB wind. The superwind radius, R_S, corresponds to when the mass loss began to increase in rate and to assume an axial as opposed to spherical symmetry. We note that our use of the term superwind is slightly modified from the intention of Iben & Renzini (1983) in that we include the symmetry change in addition to an increase in mass loss rate. The inner radius, R_{in} marks when the mass loss stopped and the size of the inner radius reflects the dynamical age that has passed since the star left the AGB (Meixner et al. 1997).

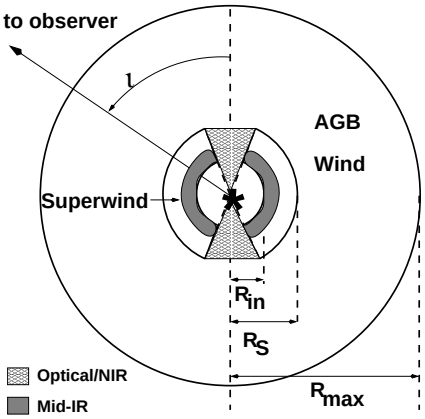

Figure 1. Schematic representation of our working model of a Proto-Planetary Nebula Dustshell.

Studies of PPN morphologies have used tracers of dust (thermal infrared radition or optical/near-infared scattered starlight) or molecular gas (CO maps or maser maps). Since the molecular gas observations are covered by others in this volume (see Huggins; Alcolea; Fong et al.), I will focus on the tracers of dust. In PPN, the central star heats the dust and the dust both scatters the starlight and radiates in the thermal infrared ($\lambda > 5\mu$m). In our working model, we expect that the scattered starlight will preferentially leak out of the lower density bipolar openings of the dustshell and will be the most intense in the inner regions where both the starlight and dust density are highest. In the thermal infrared, what we see depends on the wavelength we observe because dust radiates as a modified black body and hence depends sensitively on temperature. In these dust shells, the temperature decreases from at $\sim$200 K at the inner radius to $\sim$30 K at the outer radius. Mid-infrared (Mid-IR; 8-25μm) emission arises exclusively from the inner regions where the dust is warm. Far-IR and submillimeter radiation (>50 μm) arises from the outer regions as well as the inner regions, however, the angular resolution at these wavelengths is presently quite poor (10-40$''$) which prevents investigation of the inner, axisymmetric regions.

3.1. Mid-IR Imaging Studies

Ground based mid-IR imaging studies of PPN have had typical angular resolutions of about 1$''$ and enough spectral resolution to separate dust features and dust continuum. The larger telescopes coming on line, e.g. Keck, VLT, Gemini and MMT, promise diffraction limited performance as good as 0.$''$2 (e.g. see Morris in this volume, and Jura & Werner 2000). A number of published mid-IR imaging studies of PPN have focused on one to five well resolved PPN and usually include radiative transfer modeling (Skinner et al. 1994; Hawkins et al. 1995; Hora et al. 1996; Dayal et al. 1998; Meixner et al. 1997; Skinner et al. 1997). A recent survey paper of 66 PPNe (Meixner et al. 1999) provides the largest data base of PPNe candidate mid-IR images to date. It also incorprates the results of previously published works. Considering all the published mid-IR images to date, there are three main points that can be made (Meixner

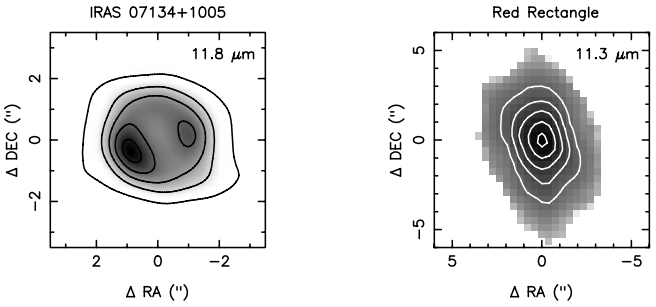

Figure 2. Mid-IR images of two types of PPNe with the wavelengths in the upper right corner. Left: IRAS 07134+1005, an example of a Toroidal PPN (Meixner et al. 1997). Right: Red Rectangle, an example of a core/elliptical (Meixner et al. 1999).

et al. 1999). First, of the 73 PPNe candidates, 33% have been resolved with $\sim 1''$ resolution. The cooler and brighter objects are easier to resolve probably because cooler shells are more distant from the central star and hence larger and brighter shells are either closer or more luminous which create larger mid-IR emission regions. Second, all of the well resolved PPNe are axisymmetric. Thirdly, there appear to be two morphological types in the well-resolved mid-IR PPNe candidates which we have called toroidal and core/elliptical. Toroidals, as exemplified by IRAS 07134+1005 (Fig. 2), have elliptical/round outer perimeters and two peaks which can be interpreted as limb brightened peaks of an equatorial density enhancement. The central star usually appears between the two peaks. Core/ellipticals, as exemplified by the Red Rectangle (Fig. 2), have tremendously bright, unresolved cores at their centers and low surface brightness elliptical shaped nebulae surrounding these cores. The extension of the low surface brightness emission is in the same direction as the optical reflection nebulosity found in these objects.

3.2. Optical Polarimetry and Imaging Studies

The optical and near-IR polarimetry and imaging observations of the scattered starlight in PPN predate (1970's) and far out number these mid-IR studies. Here I only have room to summarize some recent work. Two large survey polarimetry studies of PPN have revealed a large amount of polarization at the PPN stage which indicates that the PPN stage is axisymmetric. Using broad band polarimetry, Johnson & Jones (1991) investigated 38 objects ranging from the AGB to PPN to PN stages and found that the polarization increased from the AGB to PPN stage and then decreased in the PN stage. Using spectropolarimetry, Trammell, Dinerstein & Goodrich (1994), studied 31 PPN and found 80% had some intrinsic polarization. They also classified polarized PPN into Type 1 and Type 2. Both have large polarizations, but Type 1's also have a large position angle rotation with wavelength which suggests that Type 1's may be more bipolar in shape. See Gledhill et al. and Su et al. in this volume for recent near-IR polarimetry work on PPN.

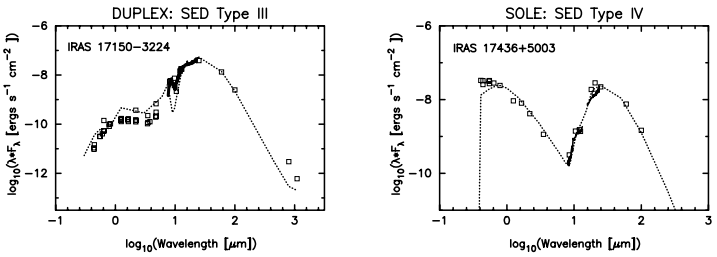

Figure 3. The spectral energy distributions for DUPLEX PPN, IRAS 17150-3224 (left) and for SOLE PPN IRAS 17436+5003 (right). Photometry data are the squares, spectroscopy the solid lines and the model in dashed lines. From Meixner et al. (2000).

High angular resolution optical and imaging studies of PPN are numerous and have exploded with use of HST because the compact nature of PPNe is well suited for HST. A number of the studies focus on one or a few objects and range from phenomenological discussions to quantitative modelling in their interpretations (e.g. Sahai, Bujarrabal & Zijlstra 1999; Sahai et al. 1999; Kwok, Su & Hrivnak 1998; Su et al. 1998; Sahai et al. 1998; Kwok et al. 1996; Skinner et al. 1997; Trammell & Goodrich 1996; Bobrowsky et al. 1995; Latter et al. 1993; in this volume see Trammell et al., Hrivnak et al., Bobrowsky et al. and Bieging et al.). Two recent papers cover a significant number of PPN and strive for a more global picture of PPN. Hrivnak et al. (1999) pursued a ground based imaging study of 10 PPN with angular resolutions of $\sim$0.″75. Ueta, Meixner & Bobrowsky (2000) imaged 27 PPN using the HST WFPC2 with angular resolutions of 0.″046 (see also Ueta et al. in this volume). If we combine the imaging results from all these papers, we find that 80% of the 44 PPN have resolvable optical reflection nebulosities and all of the well resolved reflection nebulosities are axisymmetric. While many of these studies have focused on PPN with obscured central stars, the Ueta et al. (2000) survey included many PPN with optically visible, prominent stars and they discovered two types of optical morphology in the PPN.

4. Two Types of PPN

The two types of PPN have been called DUst-Prominent Longitudinally-EXtended (DUPLEX) and Star-Obvious Low-level Elongated (SOLE) PPN (see Ueta et al. in this volume). These names describe their optical morphological appearance and their acronyms describe the two lobed structures seen in DUPLEX PPNe and the continuous structures seen in SOLE PPNe. Besides their optical appearances, DUPLEX and SOLE PPNe differ in their mid-IR morphologies: DUPLEX are core-ellipticals, while SOLE are toroidals. They also have distinctly different SEDs: DUPLEX have type II or III SEDs, while SOLE have type IV SEDs in the van der Veen et al. 1989 classification. Ueta et al. (2000) claim that the cause of these differences is the optical depth of the dust shell. SOLE nebulae have less dust optical depth than DUPLEX nebulae and, hence, the central star is visible no matter the inclination angle. They further suggest that DUPLEX PPNe may well be the precursors of bipolar PNe while SOLE

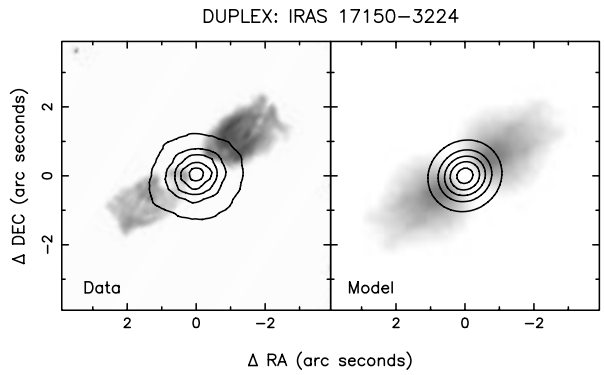

Figure 4. The model images and data for DUPLEX PPN, IRAS 17150-3224. Grayscale is the HST B band images and the contours are the 9.8μm mid-IR images. From Meixner et al. (2000).

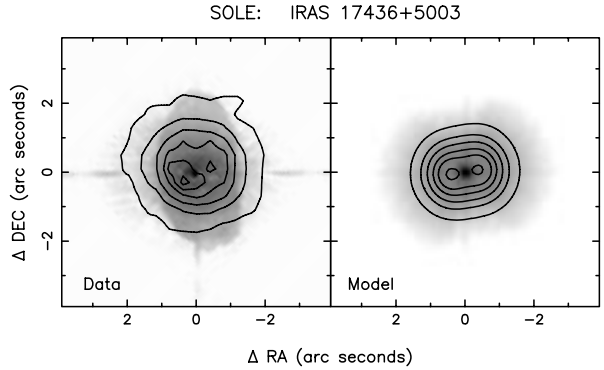

Figure 5. The model images and data for for SOLE PPN IRAS 17436+5003. Grayscale is the HST V band images and the contours are the 12.5μm mid-IR images. From Meixner et al. (2000).

PPNe may be the precursors to the elliptical PNe based on their differences in morphologies and galactic height distributions.

This interpretation is controversial, judging by the avid discussion after my talk. The other point of view, presented by Hrivnak (in this volume) is that these optical morphological differences are due primarily to inclination angle differences. That is, all these PPNe are the same physical type of beast, just viewed from different angles on the sky. The best way to resolve such controversy is to make radiative transfer models using axially symmetric dust codes to derive optical depths, and structures for all of the PPNe and compare their derived properties. Here, we present model results of one DUPLEX PPN, IRAS 17150-3224, and one SOLE PPN, IRAS 17436+5003, to demonstrate that these two sources, which are among the best examples of their classes, are physically quite different. We use a radiative transfer code that we used in Meixner et al. (1997) and Skinner et al. (1997). Su et al. (1998 and in this volume) are using a different code with similar aims but have concentrated on primarily on DUPLEX PPN so far.

We have constrained the model using our HST and mid-IR images and photometry from the literature. A full discussion of these models will appear in Meixner, Ueta & Bobrowsky (2000). Comparison of the model images and SED data demonstrates a reasonable match of the model with the data (Figs. 4 and 5). The derived parameters from the models appear in the Table and reveal the physical reasons for the apparent morphological differences. First, both objects are best fit by a 90° inclination angle; i.e. we are viewing both edge-on. Thus, we are not viewing the SOLE PPN, IRAS 17436+5003, near the pole which would be expected if our viewing angle were the main cause of the morphological differences. We note that other PPN in the Ueta et al. (2000) sample show qualitative evidence for inclination angles different than 90°; e.g. unbalanced lobes for DUPLEX and less elliptical nebulae for SOLE. Second, the optical depth for the DUPLEX PPN, IRAS 17150-3224, is significantly higher than for the SOLE PPN, IRAS 17436+5003 and explains why we do not see the central star in the former but do in the latter. The cause for the difference in optical depth is the history of mass loss. IRAS 17150-3224 experienced a more intensive mass loss rate than IRAS 17436+5003 that resulted in a denser dust cocoon of significantly higher mass. Both this higher mass and the higher luminosity for this source suggest that IRAS 17150-3224 originated from a higher mass star. These results are, of course, distance dependent and the distance maybe uncertain by a factor of two. However, the optical depth is distance independent and even with the distance uncertainty it seems reasonable to conclude that IRAS 17150-3224 is more luminous and had a higher mass progenitor.

Object	$\tau_{eq,9.7\mu m}$	incl.	$\dot{M}_{sw}$ ($M_\odot yr^{-1}$)	L_* ($L_\odot$)	D (kpc)
DUPLEX:					
IRAS 17150-3224	1.8	90°±5	50×10^{-5}	27000	3.6
SOLE:					
IRAS 17436+5003	0.9	90°±20	6×10^{-5}	3900	1.2

5. Summary points

The observational evidence from a number of independent studies clearly shows that PPNe are intrinsically axisymmetric. Thus the axisymmetry that we observe in PNe must predate the PPNe stage. Most likely the axisymmetry originates at the end of the AGB phase, because observations of the outer regions of AGB envelopes show a spherical symmetry. With the variety of PNe morphologies discussed at this conference (e.g. round, elliptical, bipolar and point symmetric), we must now begin to ask: Do we see examples of PPNe with these corresponding subtle differences in morphologies? I think we are beginning to see these differences. The DUPLEX and SOLE PPNe may well be the precursors for bipolar and elliptical PNe.

References

Balick, B. 1987, AJ, 94, 671

Bobrowsky, M. et al. 1995; ApJ, 446, L89

Dayal, A., Hoffmann, W.F., Bieging, J.H., Hora, J.L, Deutsch, L.K., & Fazio, G.G. 1998, ApJ, 492, 603

Hawkins, G.W., Skinner, C.J., Meixner, M.M., Jernigan, J.G., Arens, J.F. Keto, E., and Graham, J. 1995, ApJ, 452, 314.

Hora, J.L, Deutsch, L.K., Hoffmann, W.F., Fazio, & Giovanni, G. 1996, AJ, 112, 2064

Hrivnak, B.J. & Kwok, S. 1991, ApJ, 371, 631

Hrivnak, B.J., Kwok, S. & Volk, K. 1989, ApJ, 346, 265

Hrivnak, B.J. 1997, Proceedings of IAU Symposium No. 180, ed. Habing, H.J. & Lamers H.J.G.L.M. (Dordrecht: Kluwer Academic Publishers), p. 303

Hrivnak, B.J., Langhill, P.P., Su, K.Y.L. & Kwok, S. 1999, ApJ, 513, 421

Hu, J.Y., Slijkhuis, S., De Jong, T. & Jiang, B.W. 1993, A&AS, 100, 413

Iben, I. & Renzini, A. 1983, ARA&A, 21, 271

Jura, M. & Werner, M.W. 2000, ApJ, in press

Kwok, S. 1993, ARA&A, 31, 63

Kwok, S., Hrivnak, B.J., Zhang, C.Y., & Langhill, P.L. 1996, ApJ, 472, 287

Kwok, S., Su, K.Y.L, Hrivnak, B.J. 1998, ApJ, 501, L117

Latter, W. B., Hora, J.L., Kelly, D. M., Deutsch, L.K., & Maloney, P.R. 1993, AJ, 106, 260

Meixner, M., Skinner, C.J., Graham, J.R., Keto, E., Jernigan, J.G., & Arens, J.F. 1997, ApJ, 482, 897

Meixner et al. 1999, ApJS, 122, 221

Meixner, M., Ueta, T., & Bobrowsky, M. 2000, ApJLet., submitted

Neri, R., Kahane, C., Lucas, R., Bujarrabal, V. & Loup, C. 1998, A&AS, 122, 221

Ney, E. P., Merrill, K. M., Becklin, E. E., Neugebauer, G., Wynn-Williams, C. G. 1975, ApJ, 198, L129

Oudmaijer, R.D., van der Veen, W.E.C.J., Waters, L.B.F.M., Trams, N.R., Waelkens, C. & Engelsman, E. 1992, A&AS, 96, 625

Sahai et al. 1998, ApJ, 493, 301

Sahai, R., Bujarrabal, V. & Zijlstra, A. 1999, ApJ, 518, L115

Sahai, R., Zijlstra, A., Bujarrabal, V., Te Lintel Hekkert, P. 1999, AJ, 117, 1408

Skinner, C.J., Meixner, M.M., Hawkins, G., Keto, E., Jernigan, J.G., and Arens, J.F. 1994, ApJ, 423, L135

Skinner et al. 1997, A&A, 328, 290

Su, K.Y.L., Volk, K., Kwok, S., & Hirvnak, B.J. 1998, ApJ, 508, 744

Trammell, S.R. & Goodrich, R. W. 1996, ApJ, 468, L107

Ueta, T., Meixner, M. & Bobrowsky, M. 2000, ApJ, 528, in press

van der Veen, W.E.C.J., Habing, H.J. & Geballe, T.R. 1989, A&A, 226, 108

Van Winckel, H. 1999, Proceedings of IAU Symposium No. 191, ed. Le Betre, T., Lebre, A. & Waelkens, C. (San Francisco: ASP), p. 465